

## Sequence Distribution and Polydispersity Index Affect the Hydrogen-Bonding Strength of Poly(vinylphenol-co-methyl methacrylate) Copolymers

Chen-Lung Lin,<sup>†</sup> Wan-Chun Chen,<sup>†</sup> Chun-Syong Liao,<sup>†</sup> Yi-Che Su,<sup>†,‡</sup>  
Chih-Feng Huang,<sup>†</sup> Shiao-Wei Kuo,<sup>†</sup> and Feng-Chih Chang<sup>\*,†</sup>

*Institute of Applied Chemistry, National Chiao Tung University, Hsinchu, Taiwan, and Union Chemical Laboratories, Industrial Technology Research Institute, Hsinchu, Taiwan*

*Received March 27, 2005; Revised Manuscript Received May 19, 2005*

**ABSTRACT:** A series of poly(vinylphenol-co-methyl methacrylate) (PVPh-co-PMMA) block and random copolymers were prepared through anionic and free radical polymerizations, respectively, of 4-*tert*-butoxystyrene and methyl methacrylate and subsequent selective hydrolysis of the 4-*tert*-butoxystyrene protective groups. Analysis of infrared spectra suggests that the random copolymer possesses a higher fraction of hydrogen-bonded carbonyl groups and a larger interassociation equilibrium constant relative to those of a block copolymer containing similar vinylphenol content because of the different sequence distribution that may arise from the so-called intramolecular screening effect. In contrast, the glass transition temperature of the block copolymer, which has the lower polydispersity index, is higher than that of the random copolymer at the same composition.

### Introduction

A vast majority of the studies aimed at enhancing the miscibility of polymer blends have involved incorporating local centers into the blend components that are capable of participating in strong noncovalent interactions,<sup>1–3</sup> e.g., ion–ion interactions, ion–dipole interactions, and hydrogen-bonding interactions. In particular, several papers have emphasized the use of hydrogen bonding as a miscibility enhancer.<sup>4–7</sup> These studies indicate that the favorable hydrogen-bonding interactions are those that are stronger than the dispersive interactions that are also present; indeed, immiscible blends may be converted to single-phase materials upon introducing quite low levels of hydrogen bonding. It is well-known that the strength and extent of hydrogen bonding in copolymers or polymer blends are depended on their respective affinities<sup>8–10</sup> between the hydrogen bond donors and acceptors.

Over the years, the most widely studied hydrogen-bonding polymer blend system has been the poly(vinylphenol)/poly(methyl methacrylate) (PVPh/PMMA) blend.<sup>11–22</sup> Sermal et al.<sup>11</sup> used DSC analyses to study the phase behavior of PVPh blended with PMMA and found them to be miscible; they determined the interassociation equilibrium constant ( $K_A$ ) between the hydroxyl group of PVPh and the carbonyl group of PMMA to be 37.4. At the same time, however, Zhang et al.<sup>12</sup> reported the immiscibility of PVPh/PMMA blends from a study using the cross-polarization/magic angle spinning (CP/MAS) solid-state <sup>13</sup>C NMR spectroscopy. These contradictory observations may have arisen from the different solvents employed in the different blend preparation. The implication here is that miscibility may be achieved when methyl ethyl ketone (MEK) is used as the solvent, miscibility may be achieved, but a tetrahydrofuran (THF) cast blend is immiscible. This

phenomenon can be explained by considering that the compositional heterogeneities arise from the different solvent molecules.

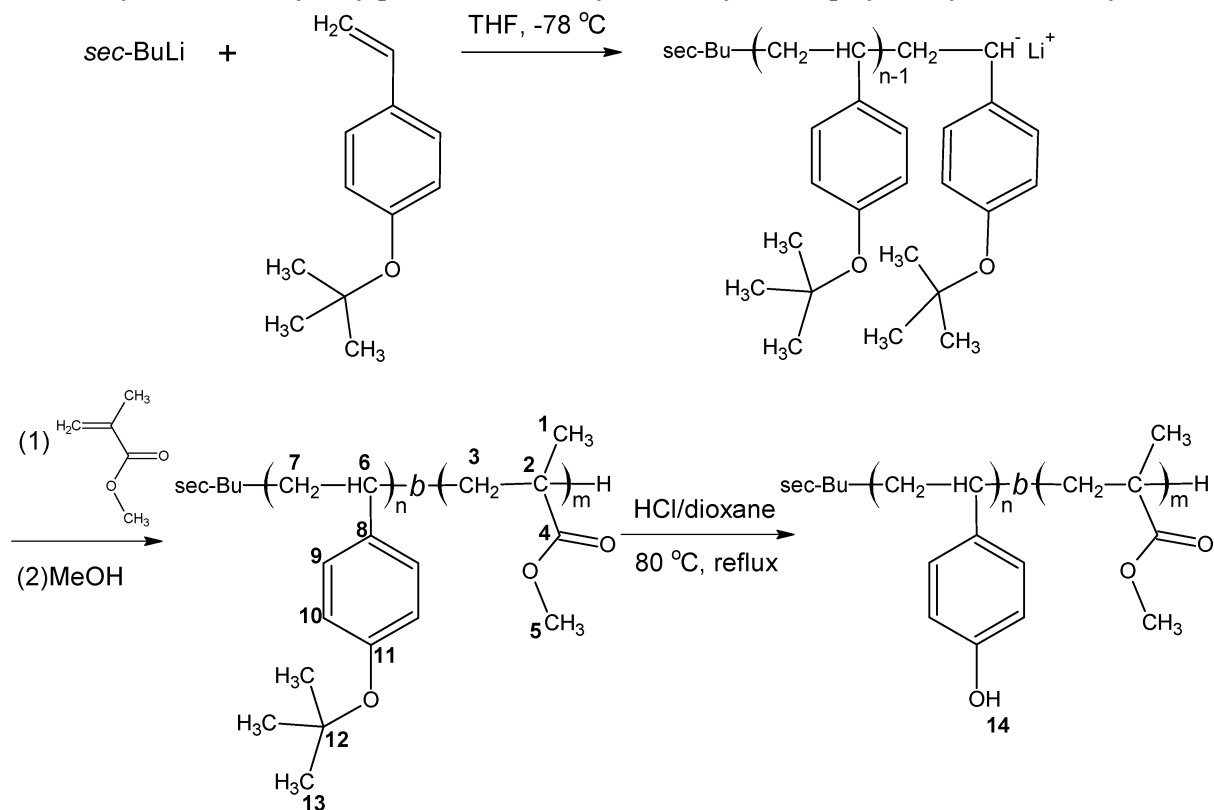
Painter and Coleman proposed<sup>23</sup> that “intramolecular screening and functional group accessibility effects” have a significant effect on the number of hydrogen-bonded functional groups. They used the FT-IR spectroscopy to measure the fraction of hydrogen-bonded carbonyl groups present in miscible blends of poly(vinylphenol) (PVPh) with poly(ethyl methacrylate) (PEMA) as a function of composition and temperature. These results have been compared to analogous ethyl methacrylate-*random*-vinylphenol (EMAVPh) copolymers, polymer solutions of PVPh and ethyl isobutyrate (EIB), and low molecular weight model mixtures of 4-ethylphenol (EPH) and EIB.<sup>24</sup> The authors found that there were significant differences in the equilibrium fractions of intermolecular hydrogen-bonded carbonyl groups that formed at identical concentrations and temperature.<sup>24</sup> Furthermore, according to the Painter–Coleman association model,<sup>2</sup> the interassociation equilibrium constant of the EMAVPh random copolymer ( $K_A = 67.4$ ) is higher than that of the PVPh/PEMA blend ( $K_A = 37.4$ ), which can be interpreted as arising from the difference in the degree of rotational freedom that results from intramolecular screening and spacing effects.<sup>23</sup> In this study, we concentrated on the effect of sequence distribution of PVPh-co-PMMA copolymer on the hydrogen-bonding strength. On the basis of our knowledge, only a few researchers<sup>25,26</sup> have compared the effects of different sequence distributions and the related hydrogen-bonding strengths of copolymers.

Katime et al.<sup>25</sup> studied the hydrogen bond strength of the poly(vinyl acetate-co-vinyl alcohol) (ACA) copolymer prepared from acidic hydrolysis; this polymer is more randomly distributed than the one obtained from basic solution. The specific interaction between the acetate carbonyl and vinyl alcohol hydroxyl groups competes with self-association of hydroxyl groups. The sequence distribution effect has been proven to be the main factor responsible for the distribution of hydrogen

<sup>†</sup> National Chiao Tung University.

<sup>‡</sup> Industrial Technology Research Institute.

\* To whom correspondence should be addressed: e-mail changfc@mail.nctu.edu.tw; Tel 886-3-5727077; Fax 886-3-5719507.

Scheme 1. Synthesis of Poly(vinylphenol-*block*-methyl methacrylate) Copolymer by Anionic Polymerization

bonds in the copolymer. Similarly, we prepared poly(vinylphenol-*co*-acetoxystyrene) copolymers of different sequence distributions through partial hydrolyses of poly(acetoxystyrene) in acidic and basic solutions. Higher glass transition temperature, higher fraction of hydrogen-bonded carbonyl groups, and a higher interassociation equilibrium constant were observed for copolymers at same composition prepared from the acidic hydrolysis than those from the basic hydrolysis because the sequence distribution of the former is relatively more random than that of the latter.<sup>26</sup> However, in these previous studies,<sup>25,26</sup> the different sequence distribution copolymers only prepared from the different hydrolyses, the real block copolymers were not available for comparison. In this paper, we describe the preparation, through anionic polymerization, of the poly(vinylphenol-*b*-methyl methacrylate) block copolymer and, through free radical polymerization, the corresponding random copolymer. We used these two copolymers to compare the specific interactions that exist within them.

### Experimental Section

**Materials.** MMA (SHOWA, 99%) and 4-*tert*-butoxystyrene (*t*BOS, Aldrich, 99%) were distilled from finely ground CaH<sub>2</sub> before use. 2,2'-Azobis(isobutyronitrile) (AIBN, SHOWA, 99%) and benzene (TEDIA, 99%) were used without further purification.<sup>27</sup> *sec*-Butyllithium (Acros, 1.3 M in cyclohexane) was used as the initiator for anionic polymerization. Tetrahydrofuran, which was used as polymerization solvent for anionic polymerization, was purified by distillation under argon from the red solution obtained by diphenylhexyllithium (produced by the reaction of 1,1-diphenylethylene and *n*-BuLi).

**Synthesis of Poly(vinylphenol-*block*-methyl methacrylate) by Anionic Polymerization.** The reactions used for the preparation of poly(vinylphenol-*block*-methyl methacrylate) (PVPh-*b*-PMMA) are shown in Scheme 1. A poly(4-*tert*-butoxystyrene-*block*-methyl methacrylate) (*Pt*BOS-*b*-PMMA) diblock copolymer was synthesized by sequential living anionic

polymerization under an inert atmosphere<sup>28</sup> in THF using *sec*-butyllithium as the initiator and degassed methyl alcohol as the terminator at  $-78\text{ }^\circ\text{C}$ . 4-*tert*-Butoxystyrene monomer was polymerized first for 2 h; an aliquot of poly(4-*tert*-butoxystyrene) was isolated for analysis after termination with degassed methanol. Methyl methacrylate monomer was then introduced into the reactor, and the reaction was terminated with degassed methanol after 2 h.

The *Pt*BOS-*b*-PMMA copolymer was converted to poly(vinylphenol-*block*-methyl methacrylate) (PVPh-*b*-MMA) through hydrolysis. The block copolymer was dissolved in dioxane, and then a 10-fold excess of 37 wt % hydrochloric acid was added. The mixture was reacted overnight at  $80\text{ }^\circ\text{C}$  under an atmosphere of argon, and then the product was precipitated into methanol/water mixture (3:7, v/v).<sup>29</sup> After neutralization with 10 wt % NaOH solution to a pH value of 6–7, the polymer was filtered off. The resulting polymer underwent two dissolve (THF)/precipitate (methanol/water) cycles and purified by the Soxhlet extraction with water for 72 h before being dried under vacuum at  $80\text{ }^\circ\text{C}$ .

Using a living anionic polymerization procedure similar to the one described above, the homopolymer of poly(vinylphenol) was synthesized to compare the thermal properties of the homopolymer with those of copolymers. In addition, the homopolymer of PMMA was polymerized at  $-78\text{ }^\circ\text{C}$  using, as the initiator, *n*-BuLi reacted with 1,1-diphenylethylene.

**Synthesis of Poly(vinylphenol-*random*-methyl methacrylate) by Free Radical Polymerization.** Solution copolymerization of methyl methacrylate with 4-*tert*-butoxystyrene in benzene was performed in glass reaction flasks containing condensers at  $70\text{ }^\circ\text{C}$  under an argon atmosphere. AIBN was employed as an initiator, and the mixture was stirred for ca. 12 h. To determine reactivity ratios, samples of the copolymers were taken from the reaction flasks in the early stage of copolymerization when the degree of conversion was low (4–9%). The copolymer was purified by repeatedly dissolving in THF and precipitating in methanol/water mixture (3:7, v/v). The synthesized poly(4-*tert*-butoxystyrene-*random*-methyl methacrylate) (*Pt*BOS-*r*-PMMA) was dissolved in dioxane at a concentration of 10% (w/v). The solution was then

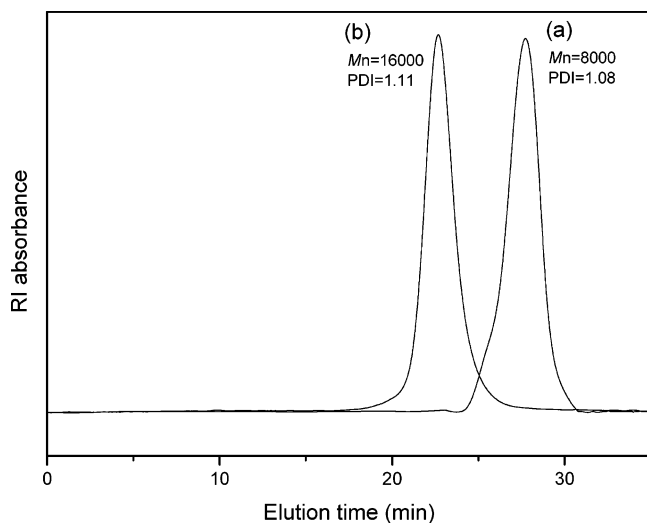


**Figure 1.** GPC traces of PVPh-*b*-PMMA block copolymers: (a) first block poly(*tert*-butoxystyrene) (PtBOS),  $M_n = 8000$  g/mol, PDI = 1.08; (b) poly(vinylphenol-*b*-methyl methacrylate) (PVPh-*b*-PMMA),  $M_n = 16\,000$  g/mol, PDI = 1.11.

refluxed overnight in the presence of 37% HCl to remove the *tert*-butoxy groups. Before vacuum drying, the poly(vinylphenol-*random*-methyl methacrylate) (PVPh-*r*-PMMA) was precipitated repeatedly from THF solution into methanol/water and purified by the Soxhlet extraction with water for 72 h to remove any residual HCl.

**Blend Preparation.** Blends of various binary PVPh/PMMA blend compositions were prepared by solution-casting. Methyl ethyl ketone (MEK) solution containing 5 wt % polymer mixture was stirred for 6–8 h, and then it was cast onto a Teflon dish. The solution was left to evaporate slowly at room temperature for 1 day. The blend films were then dried at 50 °C for 2 days.

**Measurements.** Molecular weights and molecular weight distributions were determined through GPC using a Waters 510 HPLC equipped with a 410 differential refractometer, a UV detector, and three Ultrastaygel columns (100, 500, and  $10^3$  Å) connected in series and THF as eluent at a flow rate of 0.6 mL/min and 35 °C. The molecular weight calibration curve was obtained using polystyrene standards.  $^1\text{H}$  NMR and  $^{13}\text{C}$  NMR spectra were obtained using an INOVA 500 instrument; acetone- $d_6$  was the solvent. All infrared spectra were recorded at 25 °C at a resolution of  $1\text{ cm}^{-1}$  on a Nicolet AVATAR 320 FTIR spectrometer and degassed with nitrogen. Each sample was dissolved in methyl ethyl ketone (MEK) and then cast directly onto KBr pellets. All films were vacuum-dried and were thin enough to be within the absorbance range where the Beer–Lambert law is obeyed. Thermal analysis was performed on a DSC instrument from Du-Pont (DSC-9000) at a scan rate of 20 °C/min over a temperature range from 20 to 250 °C. The sample was quenched to 20 °C from the melt state for the first scan and then rescanned between 20 and 250 °C at 20 °C/min. The glass transition temperature was obtained at the inflection point of the jump heat capacity.

## Results and Discussion

**Synthesis of Poly(vinylphenol-*block*-methyl methacrylate) Copolymer by Anionic Polymerization.** The block copolymer, PVPh-*b*-PMMA, was designed and prepared by living anionic polymerization and subsequent hydrolytic deprotection. The GPC trace of the PVPh-*b*-PMMA block copolymer obtained after polymerization and hydrolysis shown in Figure 1 displays a narrow molecular weight distribution. Although this diblock copolymer system has not been investigated previously, living anionic polymerization of the protected hydroxystyrene monomer<sup>29–31</sup> and methyl meth-

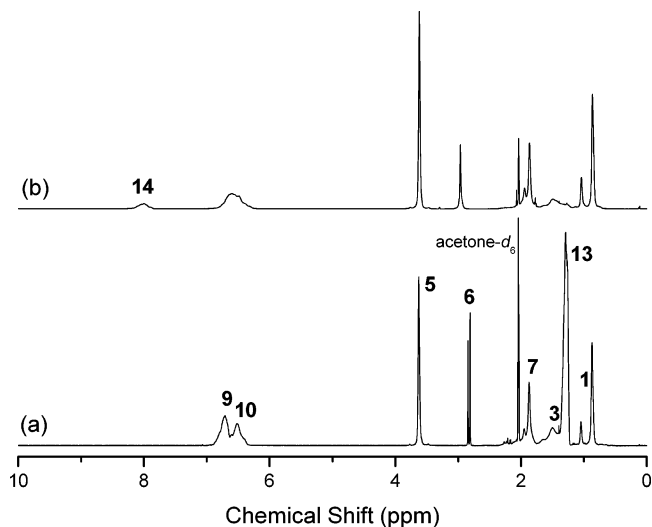


**Figure 2.**  $^1\text{H}$  NMR spectra of (a) before hydrolysis, PtBOS-*b*-PMMA, and (b) after hydrolysis, PVPh-*b*-PMMA.

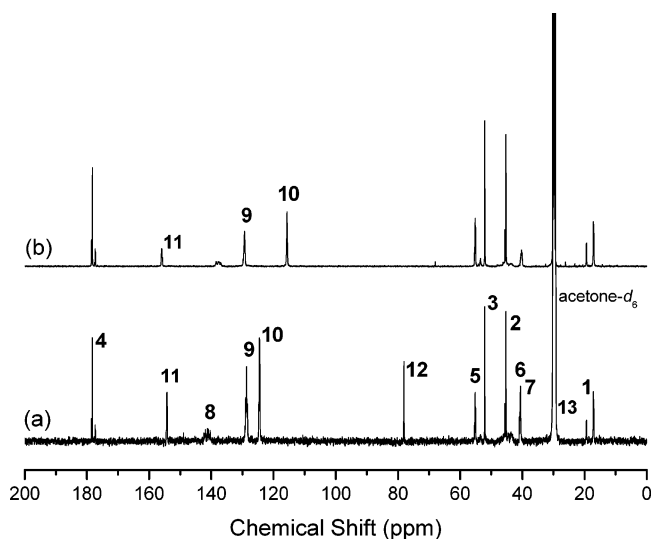


**Figure 3.**  $^{13}\text{C}$  NMR spectra of (a) before hydrolysis, PtBOS-*b*-PMMA, and (b) after hydrolysis, PVPh-*b*-PMMA.

acrylate monomer<sup>32,33</sup> are well documented. To obtain a monodisperse PVPh block, it is necessary to protect the hydroxyl group prior to polymerization to avoid the termination of the living chain end. Various protecting groups, including *tert*-butyl ether<sup>31</sup> and *tert*-butyldimethylsilyl<sup>30</sup> groups, have been used for hydroxyl group protection during anionic polymerization. In this study, the *tert*-butyl ether protected monomer was used because of its simple hydrolysis and ready availability.

The complete elimination of the protective groups and the regeneration of the phenolic hydroxyl groups were demonstrated by  $^1\text{H}$  and  $^{13}\text{C}$  NMR spectroscopy. Figure 2 displays typical  $^1\text{H}$  NMR spectra of the diblock copolymer recorded before (bottom) and after (top) deprotection. A chemical shift at 1.29 ppm corresponds to the *tert*-butyl group of the PtBOS-*b*-PMMA copolymer (in acetone- $d_6$ ). The spectrum of the hydrolyzed block copolymer essentially disappeared on those peaks corresponding to the *tert*-butyl group; only polymer backbone protons appear in the chemical shift region of 1–2 ppm. In addition, a peak (8.0 ppm) corresponding to the proton of the hydroxyl group appears after hydrolysis reaction. Figure 3 displays the  $^{13}\text{C}$  NMR spectra of the PtBOS-*b*-PMMA and PVPh-*b*-PMMA copolymers. The

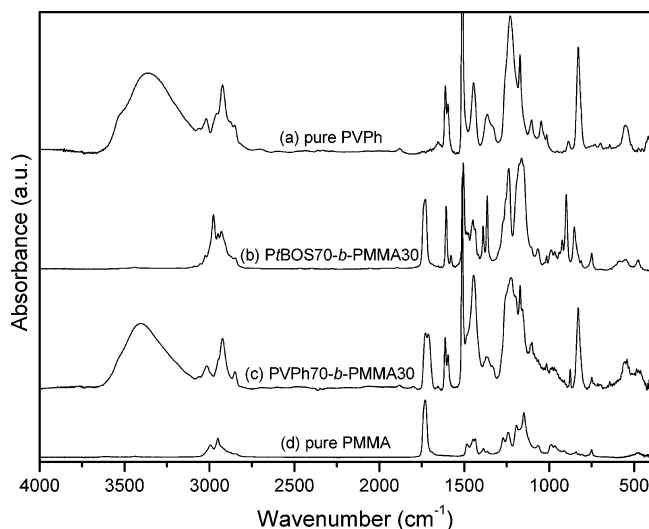


**Figure 4.** IR spectra of (a) pure PVPh, (b) PtBOS-*b*-PMMA, (c) PVPh-*b*-PMMA, and (d) pure PMMA at room temperature ranging from 400 to 4000  $\text{cm}^{-1}$ .

signal of the quarternary carbon atoms of the *tert*-butyl group in the PtBOS segment is located at 78.0 ppm. After hydrolysis reaction, no signal remains for the *tert*-butyl group (Figure 3b). Scheme 1 displays all of the other peak assignments presented in Figures 2 and 3. As mentioned above, the *tert*-butyl group was deliberately chosen as a protective group in this study because it was expected to be selectively and readily removed from the parent copolymers without hydrolyzing the methacrylate ester groups.<sup>34–36</sup> The FT-IR spectrum (Figure 4) of the resulting block copolymer after hydrolysis clearly shows the carbonyl stretching vibration band of PMMA segment in the region from 1690 and 1750  $\text{cm}^{-1}$ . The broad peak at 3450  $\text{cm}^{-1}$  in Figure 4c indicates the presence of the hydroxyl groups. The molecular weight fraction of the PVPh-*b*-PMMA block copolymer was measured by  $^1\text{H}$  NMR spectroscopy by analyzing their relative signal intensities of the protons of the PMMA and PVPh segments. The calculation was performed by comparing the signals of the aromatic protons of the PVPh segment (6.4–6.8 ppm) and the signal of the methyl ester groups of the PMMA segment (3.6 ppm). Table 1 lists these calculated molecular weight fractions and the total molecular weights determined by GPC; the number “*n*” beside the descriptor “PVPh-*b*-PMMA” reflects the molecular weight fraction.

**Synthesis of Poly(vinylphenol-random-methyl methacrylate) Copolymer through Free Radical Polymerization.** The random copolymer was prepared in benzene at 70 °C under argon using AIBN as initiator (Scheme 2). A series of random copolymers were prepared containing different MMA and *t*BOS monomer concentrations. As mentioned above, the total molecular weight of copolymer was determined by GPC, and the chemical composition of the copolymer was characterized by  $^1\text{H}$  NMR. The complete elimination of the protective groups and the regeneration of the phenolic hydroxyl groups were also demonstrated by  $^1\text{H}$  and  $^{13}\text{C}$  NMR spectroscopies using a method similar to that used for block copolymer (for brevity, not shown here), and these respective values are summarized in Table 2. Here, we assume that the PtBOS precursor and ensuing PVPh copolymer possessed the same degree of polymerization in both block and random copolymers.

To estimate copolymer composition, we used the Kelen–Tüdös method to determine the reactivity ratios ( $r_1$  and  $r_2$ ) for MMA and *t*BOS.<sup>37,38</sup> The values of  $r_1 = k_{11}/k_{12}$  and  $r_2 = k_{22}/k_{21}$  are the ratios of homo-propagation/cross-propagation rate constants for each monomer species. All polymerizations were performed in benzene under the same conditions described in the Experimental Section and terminated them below 10% monomer conversion to minimize errors due to changes in the feed ratio. This method derives the reactivity ratio from the well-known “copolymerization equation” which contains two parameters,  $\eta$  and  $\xi$ , as described in previous literature.<sup>39,40</sup> The results are displayed graphically for the PtBOS-*co*-PMMA copolymer in Figure 5, from which values of  $r_{\text{PMMA}} = 0.8$  and  $r_{\text{PtBOS}} = 0.28$  are calculated. The apparent linear relationship suggests that the copolymerization of these two comonomers follows the simple two-parameter (terminal) model. The product of the reactivity ratios falls within the range 0.18–0.25, which indicates that these two monomers are introduced into the polymer chain in an essentially random fashion with a slight tendency toward alternation. Hence, these copolymers synthesized by free radical polymerization are essentially random copolymers.

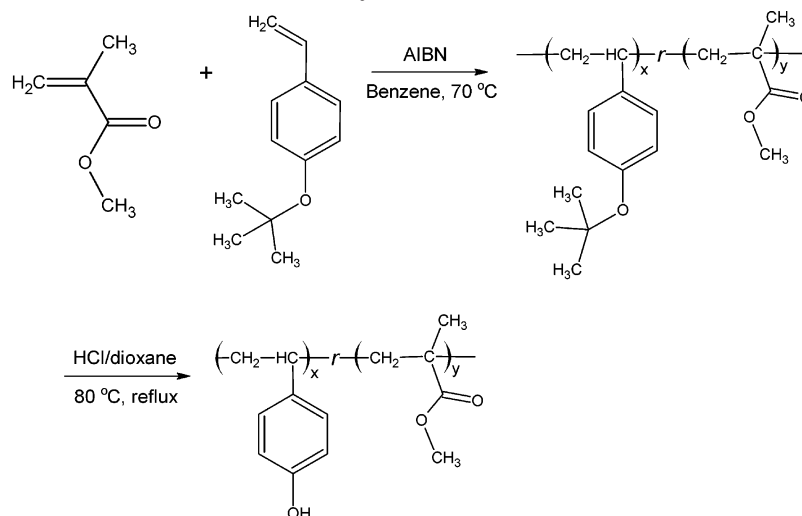
**FT-IR Analyses.** Several regions within the infrared spectra of PVPh-*co*-PMMA copolymers are influenced by hydrogen-bonding interaction. Figure 6 shows the infrared spectra in the 2700–3800  $\text{cm}^{-1}$  range for different sequence distributions of PVPh-*co*-PMMA copolymers prepared from (a) free radical and (b) anionic polymerizations in addition to (c) the PVPh/MMA blend system. Clearly, the hydroxyl stretching intensities of both copolymers and polymer blend shift to lower wavenumber upon increasing the vinylphenol content. In the meantime, the hydroxyl stretching band broadens as a result of being composed of contributions arising from the different environments surrounding the hydroxyl groups. These data suggest that there are many different types of hydroxyl groups present in PVPh-*co*-PMMA copolymers and PVPh/PMMA blends. The spectrum of pure PVPh shown in Figure 6 is characterized by a very broad band centered at 3350  $\text{cm}^{-1}$ , indicating that these hydroxyl groups are hydrogen bonded to other hydroxyl groups as dimers and chainlike multimers. A second narrower band, observed at 3525  $\text{cm}^{-1}$  as a shoulder on the high-frequency side of the broad hydrogen-bonded band, is assigned to free hydroxyl groups.<sup>2</sup> The interassociation hydrogen bonding between hydroxyl and carbonyl groups is at the middle wavenumber (depending on the sequence distribution and compositions in copolymer and compositions in polymer blend).

Taking into account the effect of composition, the carbonyl groups of methyl methacrylate units compete with self-associated hydroxyl groups for hydrogen bonding and cause the shift of the hydroxyl band toward higher wavenumbers at lower vinylphenol content. In this situation, the majority of only one type of hydroxyl group from the hydrogen–carbonyl interassociation is expected, and thus the hydroxyl stretching band is relatively narrower. In the cases of block copolymers and blend systems, this shift is less pronounced. On the contrary, the free, dimer, or multimer hydrogen-bonded hydroxyl groups will exist at higher vinylphenol contents, resulting in broader absorptions. Thus, the self-association hydrogen bonding of hydroxyl group dominates at higher vinylphenol contents.

**Table 1. Characterization of Poly(vinylphenol-*block*-methyl methacrylate) Prepared by Anionic Polymerization**

copolymer	$M_{n,PMMA}$ (g/mol) <sup>a</sup>	$M_{n,PVPh}$ (g/mol) <sup>a</sup>	total $M_n$ (g/mol) <sup>b</sup>	composition of PVPh (wt %) <sup>a</sup>	$M_w/M_n$ <sup>b</sup>	$T_g$ (°C)
PMMA	10 300		10 300	0	1.17	105
PVPh30- <i>b</i> -PMMA70	11 200	4 800	16 000	30	1.11	148
PVPh40- <i>b</i> -PMMA60	9 600	6 400	16 000	40	1.15	159
PVPh55- <i>b</i> -PMMA45	13 500	16 500	30 000	55	1.10	168
PVPh75- <i>b</i> -PMMA25	5 500	16 500	22 000	75	1.13	181
PVPh		20 000	20 000	100	1.07	181

<sup>a</sup> Obtained from <sup>1</sup>H NMR measurement. <sup>b</sup> Obtained from GPC analysis.

**Scheme 2. Synthesis of Poly(vinylphenol-*random*-methyl methacrylate) Copolymer through Free Radical Polymerization****Table 2. Characterization of Poly(vinylphenol-*random*-methyl methacrylate) Prepared by Free Radical Polymerization**

copolymer	monomer feed (mol %) <sup>a</sup>		polymer composition (mol %) <sup>a</sup>		$M_n$ (g/mol) <sup>b</sup>	$M_w/M_n$ <sup>b</sup>	$T_g$ (°C)
	<i>t</i> BOS	MMA	<i>t</i> BOS	MMA			
P <i>t</i> BOS30- <i>r</i> -PMMA70	19.6	80.4	21.0	79.0	20 600	1.64	110
P <i>t</i> BOS58- <i>r</i> -PMMA42	36.2	64.8	53.1	46.9	24 200	1.68	104
P <i>t</i> BOS76- <i>r</i> -PMMA24	57.0	43.0	72.4	27.6	24 000	1.51	101
P <i>t</i> BOS92- <i>r</i> -PMMA8	83.6	16.4	91.1	8.9	23 000	1.67	71

copolymer	$M_{n,PMMA}$ (g/mol) <sup>a</sup>	$M_{n,PVPh}$ (g/mol) <sup>a</sup>	composition of PVPh (wt %) <sup>a</sup>	$M_n$ (g/mol) <sup>b</sup>	$M_w/M_n$ <sup>b</sup>	$T_g$ (°C)
PVPh30- <i>r</i> -PMMA70	12 600	5400	30	18 000	1.62	143
PVPh58- <i>r</i> -PMMA42	8000	11 000	58	19 000	1.63	160
PVPh76- <i>r</i> -PMMA24	4200	13 400	76	17 600	1.49	169
PVPh92- <i>r</i> -PMMA8	1300	14 700	92	16 000	1.63	179

<sup>a</sup> Obtained from <sup>1</sup>H NMR measurement. <sup>b</sup> Obtained from GPC analysis.

In Figure 7, the spectra in the hydroxyl stretching region for two different sequence distributions of PVPh-co-PMMA copolymers and the PVPh/PMMA binary blend are displayed. There is a clear difference between the spectra of these two copolymers and the blend system, even though they possess similar vinylphenol content. The random copolymer prepared from free radical polymerization presents its hydroxyl stretching band shifted to higher wavenumber. In contrast, the hydroxyl bands of block copolymer and binary blend are relatively closer to that of pure PVPh. This can be explained in terms of different environments experienced by these hydroxyl groups. In block copolymer and binary blend, the hydroxyl environment is closer to that of PVPh, where these hydroxyl groups are surrounded mostly by other hydroxyl groups, and thus multiple self-associations are favored. It is well-known that multiple hydrogen bonding between hydroxyl groups leads to lower its wavenumber. In addition, for the random PVPh-*r*-PMMA copolymers, the absorption peak of the

broad band representing the self-associated hydroxyl-hydroxyl units shifts to higher wavenumber upon increasing PMMA content (Figure 6a). Therefore, it is reasonable to assign the band at 3440 cm<sup>-1</sup> to the hydroxyl groups interacting with carbonyl groups because the small number of the hydroxyl groups tends to interact completely with carbonyl group. Moreover, the appearance of the hydroxyl band of the random copolymer was narrower than those of block copolymer and binary blend because the existence of nearly only one type of interassociation of hydroxyl-carbonyl in the PVPh-*r*-PMMA copolymer.

The carbonyl stretching band for PMMA appears at 1730 cm<sup>-1</sup>. For PVPh-co-PMMA copolymers, Figure 8 indicates that the location of this band changes widely depending on the composition and sequence distribution of its repetitive units. The spectra of PVPh-*r*-PMMA, PVPh-*b*-PMMA, and PVPh/PMMA blend were measured at room temperature over the region from 1670 to 1760 cm<sup>-1</sup>. Again, the peaks at 1730 and 1705 cm<sup>-1</sup>,

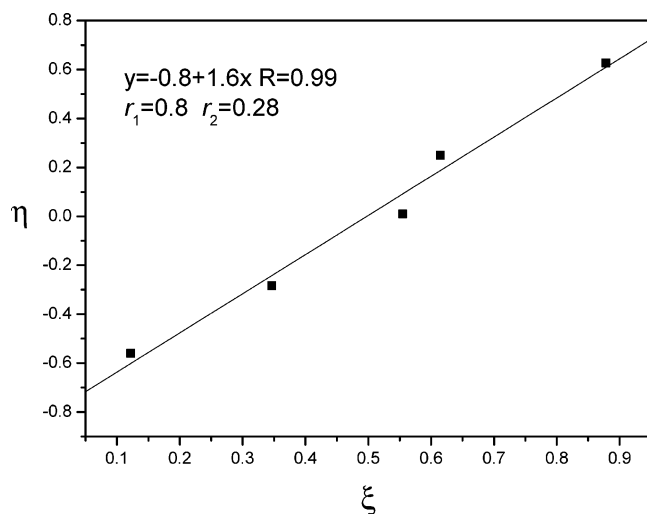


**Figure 5.** Kelen–Tüdös plot for the PtBOS-*r*-PMMA copolymers.

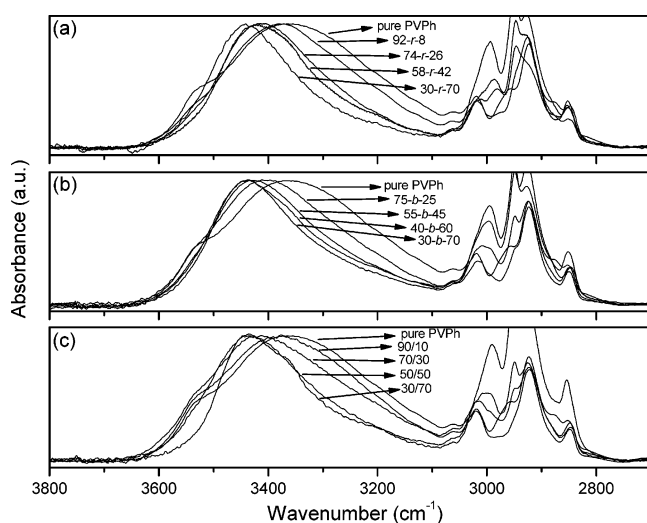


**Figure 6.** FT-IR spectra in the 2700–3800  $\text{cm}^{-1}$  region for (a) random copolymer, (b) block copolymer, and (c) polymer blend.

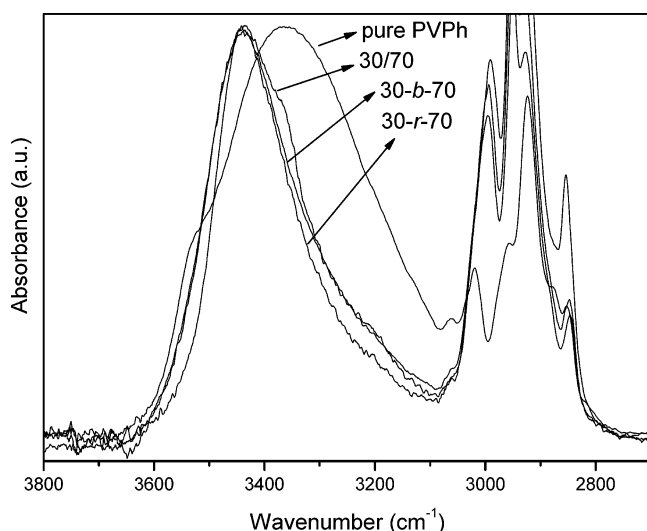


**Figure 7.** Comparison between the FTIR spectra (2700–3800  $\text{cm}^{-1}$ ) of samples having similar PVPh contents.

corresponding to the free carbonyl and hydrogen-bonded carbonyls, can be fitted well to the Gaussian function. As expected, a higher content of vinylphenol units

results in a higher number of hydrogen-bonded carbonyl groups. To obtain the fraction of the hydrogen-bonded carbonyl group, the known absorptivity ratio for hydrogen-bonded and free carbonyl contributions is required. We employed a value of  $\alpha_{\text{HB}}/\alpha_{\text{F}} = 1.5$ , which was previously calculated by Moskala et al.<sup>41</sup> Table 3 summarizes the fractions of hydrogen-bonded carbonyl groups that are calculated through curve fitting of the data from both the copolymers and the binary blends. The fraction of hydrogen-bonded carbonyl groups increased upon increasing the PVPh content for both two PVPh-*co*-PMMA copolymers and PVPh/PMMA blend system. Moreover, the fraction of hydrogen-bonded carbonyl groups of these two copolymers was always higher than that of blend system at similar PVPh contents. This observation can be explained in terms of the difference in degree of rotational freedom between polymer blend and copolymers. The polymer chain architecture of a homopolymer is significantly different from a copolymer as a result of intramolecular screening and functional group accessibility caused by the chain connectivity.<sup>42–46</sup> The PVPh segments in the PVPh/PMMA blend have more contacts with segments of its own type than exist in the corresponding copolymer because of chain connectivity and intramolecular screening effect. Intramolecular screening results from an increase in the number of same-chain contacts due to the polymer chains bending back upon themselves. This “screening” reduces the number of intermolecular hydrogen bonds that are formed in a polymer blend. Thus, the density of interassociation hydrogen bonds of a polymer blend is relatively lower than that of a corresponding copolymer. Moreover, the spacing between functional groups along a homopolymer chain and the presence of bulky side group are also responsible for the observed less interassociation hydrogen bond density in terms of the so-called functional group accessibility effect. This effect occurs as the result of steric crowding and shielding.<sup>45</sup> As a result, the density of the hydrogen-bonded carbonyl group in the PVPh/PMMA blend is relatively lower than that in the corresponding PVPh-*co*-PMMA copolymer at the same composition as would be expected.

Now, we turn our attention to a different sequence distribution of PVPh-*co*-PMMA. The fraction of hydrogen-bonded carbonyl of the PVPh-*r*-PMMA is observed to be higher than that of the block copolymer over the entire compositions. A random distributed PVPh-*r*-PMMA copolymer provides greater opportunity for hydrogen bond formation between the hydroxyl group of PVPh and the carbonyl group of PMMA than does a block copolymer. On the basis of the Painter–Coleman association model, the interassociation equilibrium constants of PVPh-*co*-PMMA copolymers prepared through both free radical and anionic polymerization were determined. The interassociation equilibrium constants ( $K_{\text{A}}$ ) of PVPh-*r*-PMMA and the PVPh/PMMA blend have been reported<sup>23</sup> to be 67.4 and 37.4, respectively. To calculate the interassociation equilibrium constant of PVPh-*b*-PMMA copolymer, the methodology of a least-squares method has been described in the previous study.<sup>47</sup> Table 4 lists all of the thermodynamic parameters in these copolymer and polymer blend systems.  $K_{\text{2}}$  and  $K_{\text{B}}$  represent the hydrogen-bonded dimer and multimer of the self-association equilibrium constants of PVPh, respectively. The  $K_{\text{A}}$  is the equilibrium constant describing the interassociation of PMMA

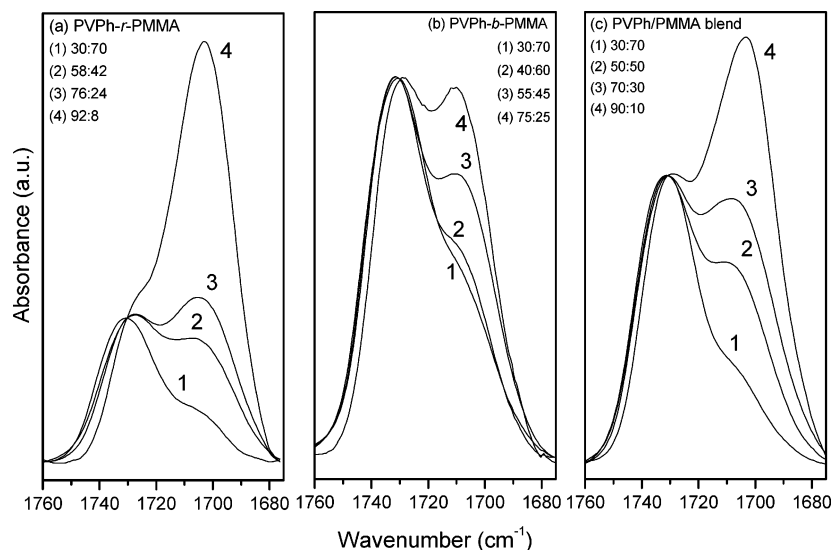


**Figure 8.** FT-IR spectra (1670–1760  $\text{cm}^{-1}$ ) of a (a) random copolymer, (b) block copolymer, and (c) polymer blend.

**Table 3. Results of Curve-Fitting the Data for PVPh-co-PMMA and PVPh/PMMA Blends at Room Temperature**

PVPh-random-PMMA	H-bonded C=O			free C=O			$f_b^a$
	$\nu$ , $\text{cm}^{-1}$	$W_{1/2}$ , $\text{cm}^{-1}$	$A_b$ , %	$\nu$ , $\text{cm}^{-1}$	$W_{1/2}$ , $\text{cm}^{-1}$	$A_b$ , %	
30–70	1707	24	35.6	1731	19	64.4	26.9
58–42	1705	26	59.3	1731	19	40.7	49.3
76–24	1704	25	75.7	1730	19	24.3	65.6
92–8	1703	24	82.3	1729	18	17.7	75.7
PVPh-block-PMMA	H-bonded C=O			free C=O			$f_b$
	$\nu$ , $\text{cm}^{-1}$	$W_{1/2}$ , $\text{cm}^{-1}$	$A_b$ , %	$\nu$ , $\text{cm}^{-1}$	$W_{1/2}$ , $\text{cm}^{-1}$	$A_b$ , %	
30–70	1709	23	32.8	1732	20	67.2	24.6
40–60	1709	24	42.1	1732	19	57.9	32.6
55–45	1708	24	58.3	1733	19	41.7	43.5
75–25	1709	25	65.8	1732	18	34.2	56.2
PVPh/PMMA blend	H-bonded C=O			free C=O			$f_b$
	$\nu$ , $\text{cm}^{-1}$	$W_{1/2}$ , $\text{cm}^{-1}$	$A_b$ , %	$\nu$ , $\text{cm}^{-1}$	$W_{1/2}$ , $\text{cm}^{-1}$	$A_b$ , %	
30–70	1707	23	24.8	1732	20	75.2	18.1
50–50	1707	25	49.7	1733	19	50.3	37.7
70–30	1707	26	58.7	1733	20	41.3	48.6
90–10	1705	24	68.5	1732	18	31.5	59.2

<sup>a</sup>  $f_b$ : fraction of hydrogen-bonded carbonyl group.

**Table 4. Summary of the Self-Association and Interassociation Parameters of PVPh-co-PMMA Copolymer and PVPh/PMMA Blend Systems**

polymer	molar vol (mL/mol)	mol wt (g/mol)	solubility parameter (cal/mL) <sup>0.5</sup>	self-association equilibrium constant		interassociation equilibrium constant $K_A$		
				$K_2$	$K_B$	random copolymer	block copolymer	polymer blend
PVPh	100.0	120.0	10.6	21.0	66.8			
PMMA	84.9	100.0	9.1			67.4	47.1	37.4

with PVPh. Accordingly, the interassociation constant of the PVPh-*b*-PMMA is obtained as 47.1 when using least-squares fit based on the fraction of hydrogen-bonded carbonyl group experimentally obtained.

Using values of  $K_A$  together with the PVPh self-association equilibrium constants ( $K_2$  and  $K_B$ ), we can calculate the theoretical curves for the number of hydrogen-bonded carbonyl group at 25 °C as a function of the weight fraction of PVPh content, and the results are displayed in Figure 9. At first sight, the shape of the calculated curve reproduces the trend in the experimental data very well. However, the fit between calculated and experimental results at high and low fractions of PVPh, i.e., at weight fractions less than 0.4, is not

quite as good it is in the central region. This derivation is reasonable because the most accurate range for determining fraction of hydrogen-bonded carbonyl groups spectroscopically is that from 0.4 to 0.7, where the bands for both free and hydrogen-bonded carbonyl groups are well separated with significant absorbance.<sup>43</sup> Outside this range of 0.4–0.7, one of the bands is buried under the other and appears as a less defined shoulder. Moreover, it can be seen from Figure 9 that the fraction of hydrogen-bonded carbonyl groups is most sensitive to the magnitude of  $K_A$  at PVPh weight fraction of >40%. Below this weight fraction, the variation of fraction of hydrogen-bonded carbonyl groups with  $K_A$  is relatively insensitive.

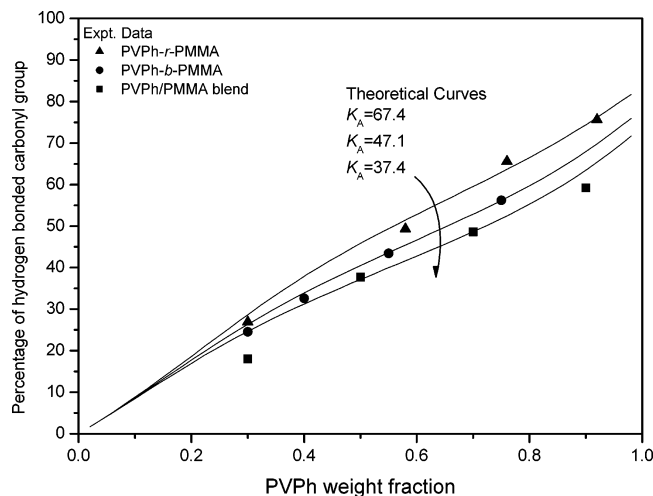


**Figure 9.** Plots of the fraction of hydrogen-bonded carbonyl groups vs the PVPh fraction for a random, block copolymer, and polymer blend.

From Table 4, the observed interassociation equilibrium constants from the PVPh-*r*-PMMA copolymer (67.4) and the self-association constant of PVPh homopolymer (66.8) are fairly close. The competition between self-associating and interassociating bonds is complicated, and numbers of self-association and inter-association hydrogen bonds depend on the component fraction in the copolymer. In addition, the interassociation equilibrium constant of the PVPh-*b*-PMMA is substantially less than that of the self-association equilibrium constant of the PVPh homopolymer (47.1 vs 66.8), which implies that the tendency toward forming hydrogen bonds between two hydroxyl groups dominates over hydroxyl-carbonyl interactions in PVPh-*b*-PMMA copolymer. Most importantly, the  $K_A$  value of PVPh-*r*-PMMA is greater than that of PVPh-*b*-PMMA copolymer, implying that the hydroxyl groups in the random copolymer have a better opportunity to interact with carbonyl groups than they do in the block copolymer. As mentioned above, and previously in the literature,<sup>42,48</sup> the intramolecular screening effect arises as a consequence of chain connectivity; the covalent linkages between polymer segments from a copolymer induce greater numbers of the same chain contacts than that calculated on the basis of a simple random mixing of segments. Hence, Painter and Coleman modified their Painter-Coleman association model (PCAM). A parameter,  $\gamma$ , was introduced, defined as the fraction of same chain contacts that originate from the polymer chain bending back upon itself, primarily through local but also through long-range connectivity effects. In brief, the equilibrium constants  $\tilde{K}_B$  and  $\tilde{K}_A$  were substituted for  $K_B$  and  $K_A$  and defined as

$$\tilde{K}_B = K_B \left[ \frac{\gamma + (1 - \gamma)\Phi_B}{\Phi_B} \right] \quad (1)$$

$$\tilde{K}_A = K_A \left[ \frac{1 - (\gamma + (1 - \gamma)\Phi_B)}{\Phi_A} \right] = K_A(1 - \gamma) \quad (2)$$

where  $\Phi_B$  and  $\Phi_A$  are the volume fraction of self-association species B (PVPh) and non-self-association species A (PMMA), respectively.  $\gamma$  is the fraction of intrachain contacts, as mentioned above. This means that  $\tilde{K}_A$  is the “effective” equilibrium constant. To adjust

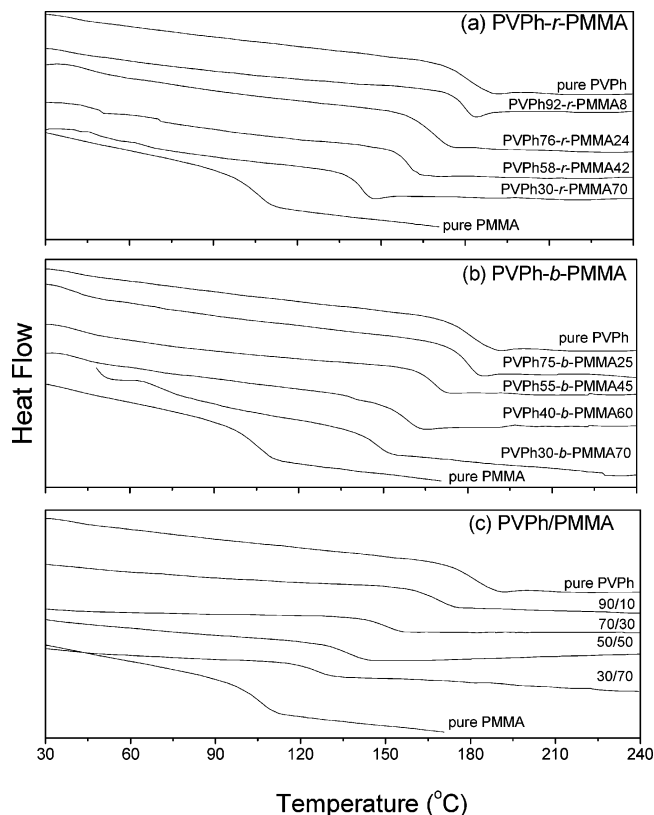


**Figure 10.** DSC traces of (a) PVPh-*r*-PMMA copolymers, (b) PVPh-*b*-PMMA copolymers, and (c) PVPh/PMMA blend.

for intramolecular screening, Painter and Coleman employed eqs 1 and 2 with a value of  $\gamma = 0.30$ , which appears most appropriate for an amorphous polymer melt.<sup>42</sup> When a value of  $\tilde{K}_A$  of 47.1 is employed for PVPh-*b*-PMMA in eq 2, the value of  $K_A$  is obtained to be 67.3 (i.e.,  $K_A = \tilde{K}_A/\gamma = 47.1/0.7$ ). In other words,  $K_A = 67.3$  of PVPh-*b*-PMMA can be considered to be the characteristic of an interassociation equilibrium constant in the absence of intramolecular screening. It is interesting to notice that this value of  $K_A = 67.3$  is very close to the value of 67.4 obtained experimentally from the PVPh-*r*-PMMA copolymer. Accordingly, it implies that the  $\tilde{K}_A$  value of a block copolymer containing both hydrogen-bonded donor and acceptor segments may be able to be estimated from the “effective” equilibrium constant of its corresponding random copolymer. While additional work is necessary to ensure the validity of such an approach, this result is not simply a fortuitous one, and it does offer the tantalizing possibility that the value of the interassociation equilibrium constant may be transformable.

**Thermal Analyses.** Differential scanning calorimetry (DSC) is a convenient method to observe thermal characteristics arising from different interactions between copolymers and polymer blends. Figure 10 shows the DSC thermograms of both PVPh-*co*-PMMA copolymers and PVPh/PMMA blend, revealing that essentially all DSC traces possess only one glass transition temperature. Single glass transition temperature strongly suggests that these systems are fully miscible and possess a homogeneous amorphous phase. The values of glass transition temperatures and  $T_g$  breadths obtained from systems are listed in Table 5. In general, a miscible polymer blend generally gives a broader DSC transition, while those of copolymer systems are relatively narrower. The random copolymer usually exhibits



**Table 5. Values of  $T_g$  and  $T_g$  Breadth Obtained from PVPh-co-PMMA Copolymer and PVPh/PMMA Blend Systems**

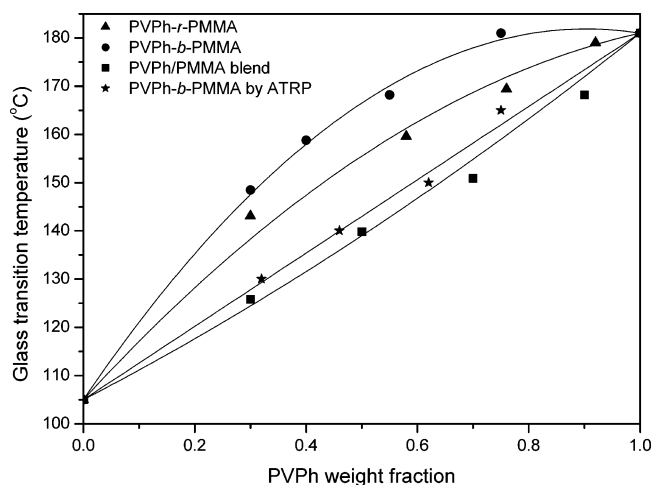
	$T_g$ (°C)	$\Delta T_g$ (°C)
PVPh-random-PMMA		
0/100	105	12.6
30/70	143	7.3
58/42	160	6.0
76/24	169	7.0
92/8	179	7.0
100/0	181	14.6
PVPh-block-PMMA		
0/100	105	12.6
30/70	149	10.0
40/60	159	8.6
55/45	168	8.6
75/25	181	7.8
100/0	181	14.6
PVPh/PMMA blend		
0/100	105	12.6
30/70	133	14.8
50/50	142	14.4
70/30	151	12.7
90/10	165	12.3
100/0	181	14.6

**Table 6. Values of  $T_g$  Obtained from the Narrow Polydispersity of PVPh**

$M_n$ (g/mol)	$M_w/M_n$	$T_g$ (°C)
3 200	1.12	174
6 000	1.14	178
20 000	1.07	181
30 000	1.06	183
150 000	1.09	186

the narrowest  $T_g$  breadth because of the more adjacent units of segments A and B. As a result, a random copolymer has greater homogeneity at the molecular scale than a block copolymer.

At the first sight, the glass transition temperatures in all systems increase upon increasing the content of vinylphenol because PVPh has a higher  $T_g$ . In another aspect, the PVPh/PMMA blend system typically has the lowest  $T_g$  at every composition. It is quite unexpected to notice that the glass transition temperature of the block copolymer is higher than that of the random copolymer containing the same PVPh content even though the fraction of hydrogen-bonded carbonyl and the value of  $K_A$  obtained from PVPh-*r*-PMMA copolymers are higher than these obtained from the PVPh-*b*-PMMA copolymers; the  $T_g$  relationship between two copolymer containing different sequence distribution does not obey the conventional trend. In general, the glass transition temperature is dependent not only on the specific interactions but also on the physical and chemical nature of the polymer molecules such as molecular weight, polydispersity, chain segment flexibility, branching, and cross-linking. It has been well documented that, for a constant polydispersity, as the molecular weight of a polymer is increased, there is a subsequent increase in glass transition temperature.<sup>49</sup> However, once a sufficiently high molar mass is obtained, the  $T_g$  remains essentially constant. This phenomenon can be rationalized by the reduction in free volume as the number of chain ends decreases with increasing molar mass. As expected, a similar trend is observed in these synthesized PVPh homopolymers (Table 6). From Table 6, it can be seen that the  $T_g$  reaches a plateau value above a molecular weight of 6000. Furthermore, these copolymers used in this study have the similar molecular weight. The influence of

**Figure 11. Plots of  $T_g$  vs composition based on (symbol) experimental data.**

molecular weight would not be the significant factor for the property of glass transition temperature. Thus, such unexpectedly result may arise from the different polydispersity between the random and the block copolymer.

It is well-known that block copolymers prepared from anionic polymerization have a lower polydispersity (ca. 1.05–1.2) than do those obtained through conventional free radical copolymerization. Higher polydispersity may result in additional interaction energy arising from the longer chain and higher radius of gyration, both of which influence polymer packing to increase in free volume and result in lower glass transition temperature.<sup>50,51</sup> To confirm this assumption, we purposely synthesized (see Supporting Information) PVPh-*b*-PMMA block copolymers of higher polydispersity by using atom transfer radical polymerization (ATRP). The synthesized PVPh-*b*-PMMA copolymer by ATRP indeed has greater polydispersity index (near the magnitude of 1.6) than that from anionic polymerization because of the purity of monomers. Although the ATRP block copolymer and anionic block copolymer were hydrolyzed under different conditions, the PtBOS and PAS segments were completely hydrolyzed and purified by the Soxhlet extraction to remove any residual NaOH or HCl. We supposed that the different hydrolysis reactions would not influence the glass transition temperature of different block copolymers.

Figure 11 shows the glass transition temperatures of each system. Again, the PVPh-*b*-PMMA copolymer obtained through anionic polymerization has the largest  $T_g$  among all of these PVPh-co-PMMA copolymers, even though its  $f_b$  and  $K_A$  are less than those of PVPh-*r*-PMMA copolymer. As mentioned previously, glass transition temperature of a polymer is strongly depended on the polydispersity index. When the PVPh-*r*-PMMA prepared by free radical polymerization and PVPh-*b*-PMMA prepared by ATRP have the similar polydispersity index, the typical trend of large value of  $f_b$  resulting in a higher value of  $T_g$  remains valid. However, the PVPh-*b*-PMMA with similar composition and molecular weight but the lowest polydispersity index results in the highest glass transition temperature.

## Conclusions

The block copolymer PVPh-*b*-PMMA and random copolymer PVPh-*r*-PMMA were designed and synthesized by anionic and free radical copolymerization of

4-*tert*-butoxystyrene and methyl methacrylate, and the *tert*-butoxy protective group was selectively removed through hydrolysis reaction. These two PVPh-*co*-PMMA copolymers, which possess the same composition but different sequence distributions, exhibit different properties. Moreover, the fractions of hydrogen-bonded carbonyl groups and glass transition temperatures of two copolymers are higher than those of the PVPh/PMMA blend system at similar PVPh content. This observation can be attributed to the difference in degrees of rotational freedom between polymer blend and copolymer. Meanwhile, the polymer chain architecture of a homopolymer is significantly different from that of copolymers due to intramolecular screening and functional group accessibility caused by the covalent bond connectivity. In addition, the interassociation equilibrium constant of PVPh-*r*-PMMA copolymer obtained from curve fitting method of  $f_i$  and based on PCAM is larger than that of PVPh-*b*-PMMA copolymer.  $K_A = 67.3$  of the PVPh-*b*-PMMA without intramolecular screening is very close to the value of 67.4 obtained experimentally from the PVPh-*r*-PMMA copolymer. This result provides us with a hint that the effective interassociation equilibrium constant may be transformed between block copolymer and random copolymer that contained the same hydrogen-bonded donor and acceptor segment. The block copolymer has the highest  $T_g$  value because it has the lowest polydispersity index.

**Acknowledgment.** This research was financially supported by the National Science Council, Taiwan, Republic of China, under Contract NSC-93-2216-E-009-018.

**Supporting Information Available:** Synthetic and characterization details of PVPh-*b*-PMMA block copolymer through ATRP, including FT-IR and NMR spectra and DSC thermograms. This material is available free of charge via the Internet at <http://pubs.acs.org>.

## References and Notes

- Utracki, L. A. *Polymer Alloys and Blends: Thermodynamics and Rheology*; Carl Hanser Verlag: Munich, 1989.
- Coleman, M. M.; Graf, J. F.; Painter, P. C. *Specific Interactions and the Miscibility of Polymer Blends*; Technomic Publishing: Lancaster, PA, 1991.
- Coleman, M. M.; Painter, P. C. *Prog. Polym. Sci.* **1995**, *20*, 1.
- Coleman, M. M.; Lee, J. Y.; Serman, C. J.; Wang, Z.; Painter, P. C. *Polymer* **1989**, *30*, 1298.
- Serman, C. J.; Xu, Y.; Painter, P. C.; Coleman, M. M. *Polymer* **1991**, *32*, 516.
- Kuo, S. W.; Chang, F. C. *Macromolecules* **2001**, *34*, 4089.
- Kuo, S. W.; Chang, F. C. *Macromolecules* **2001**, *34*, 5224.
- He, Y.; Zhu, B.; Inoue, Y. *Prog. Polym. Sci.* **2004**, *29*, 1021.
- Kuo, S. W.; Huang, C. F.; Chang, F. C. *J. Polym. Sci., Polym. Phys.* **2001**, *39*, 1348.
- Kuo, S. W.; Lin, C. L.; Chang, F. C. *Polymer* **2002**, *43*, 3943.
- Serman, C. J.; Painter, P. C.; Coleman, M. M. *Polymer* **1991**, *32*, 1049.
- Zhang, X.; Takegoshi, K.; Hikichi, K. *Macromolecules* **1991**, *24*, 5756.
- Li, D.; Brisson, J. *Macromolecules* **1996**, *29*, 868.
- Dong, J.; Ozaki, Y. *Macromolecules* **1997**, *30*, 286.
- Serman, C. J.; Xu, Y.; Painter, P. C.; Coleman, M. M. *Macromolecules* **1989**, *22*, 2015.
- Li, D.; Brisson, J. *Polymer* **1998**, *39*, 793.
- Li, D.; Brisson, J. *Polymer* **1998**, *39*, 801.
- Hsu, W. P. *J. Appl. Polym. Sci.* **2002**, *83*, 1425.
- Jong, L.; Pearce, E. M.; Kwei, T. K. *Polymer* **1993**, *34*, 48.
- Hsu, W. P.; Yeh, C. F. *J. Appl. Polym. Sci.* **1999**, *73*, 431.
- Xu, Y.; Graf, J.; Painter, P. C.; Coleman, M. M. *Polymer* **1991**, *32*, 3103.
- Wang, L. F.; Pearce, E. M.; Kwei, T. K. *J. Polym. Sci., Polym. Phys. Ed.* **1991**, *29*, 619.
- Painter, P. C.; Coleman, M. M. *Polymer Blends*; Paul, D. R., Ed.; John Wiley & Sons: New York, 2000; Vol. 1.
- Coleman, M. M.; Xu, Y.; Painter, P. C. *Macromolecules* **1994**, *27*, 127.
- Isasi, J. R.; Cesteros, L. C.; Katime, I. *Macromolecules* **1994**, *27*, 2200.
- Kuo, S. W.; Liu, W. P.; Chang, F. C. *Macromolecules* **2003**, *36*, 5165.
- Sybert, P. D.; Beever, W. H.; Stille, J. K. *Macromolecules* **1981**, *14*, 493.
- Ndoni, S.; Papadakis, C. M.; Bates, F. S.; Almdal, K. *Rev. Sci. Instrum.* **1995**, *66*, 1090.
- Li, M.; Douki, K.; Goto, K.; Li, X.; Coenjarts, C.; Smilgies, D. M.; Ober, C. K. *Chem. Mater.* **2004**, *16*, 3800.
- Zhao, J. Q.; Pearce, E. M.; Kwei, T. K.; Jeon, H. S.; Kesani, P. K.; Balsara, N. P. *Macromolecules* **1995**, *28*, 1972.
- Se, K.; Miyawaki, K.; Hirahara, K.; Takano, A.; Fujimoto, T. *J. Polym. Sci., Polym. Chem.* **1998**, *36*, 3021.
- Hadjichristidis, N.; Iatrou, H.; Pispas, S.; Pitsikalis, M. *J. Polym. Sci., Polym. Chem.* **2000**, *38*, 3212.
- Jérôme, R.; Teyssié, Ph.; Vuillemin, B.; Zundel, T.; Zune, C. *J. Polym. Sci., Polym. Chem.* **1999**, *37*, 1.
- Kurita, K.; Inoue, M.; Harata, M. *Biomacromolecules* **2002**, *3*, 147.
- Mecerreyes, D.; Moineau, G.; Dubois, P.; JeÂroÂme, R.; Hedrick, J. L.; Hawker, C. J.; Malmström, E. E.; Trollsas, M. *Angew. Chem., Int. Ed.* **1998**, *37*, 1274.
- Heise, A.; Hedrick, J. L.; Frank, C. W.; Miller, R. D. *J. Am. Chem. Soc.* **1999**, *121*, 8647.
- Kennedy, J. P.; Kelen, T.; Tüdös, F. *J. Polym. Sci., Polym. Chem. Ed.* **1975**, *13*, 2277.
- Kelen, T.; Tüdös, F. *J. Macromol. Sci., Chem.* **1975**, *A9*, 1.
- Kuo, S. W.; Chang, F. C. *Polymer* **2001**, *42*, 9843.
- Xu, Y.; Painter, P. C.; Coleman, M. M. *Polymer* **1993**, *34*, 3010.
- Moskala, E. J.; Howe, S. E.; Painter, P. C.; Coleman, M. M. *Macromolecules* **1984**, *17*, 1671.
- Painter, P. C.; Veytsman, B.; Kumar, S.; Shenoy, S.; Graf, J. F.; Xu, Y.; Coleman, M. M. *Macromolecules* **1997**, *30*, 932.
- Coleman, M. M.; Pehlert, G. J.; Painter, P. C. *Macromolecules* **1996**, *29*, 6820.
- Pehlert, G. J.; Painter, P. C.; Veytsman, B.; Coleman, M. M. *Macromolecules* **1997**, *30*, 3671.
- Pehlert, G. J.; Painter, P. C.; Coleman, M. M. *Macromolecules* **1998**, *31*, 8423.
- Coleman, M. M.; Guigley, K. S.; Painter, P. C. *Macromol. Chem. Phys.* **1999**, *200*, 1167.
- Kuo, S. W.; Chang, F. C. *Macromol. Chem. Phys.* **2001**, *202*, 3112.
- Coleman, M. M.; Painter, P. C. *Macromol. Chem. Phys.* **1998**, *199*, 1307.
- Fox, A.; Loshaek, S. *J. Polym. Sci.* **1955**, *15*, 371.
- Sperling, L. H. *Introduction to Physical Polymer Science*, 3rd ed.; John Wiley & Sons: New York, 2001.
- Barclay, G. G.; Hawker, C. J.; Ito, H.; Orellana, A.; Malenfant, P. R. L.; Sinta, R. F. *Macromolecules* **1998**, *31*, 1024.

MA050639T